

# A Systematic Benchmarking of $^{31}\text{P}$ and $^{19}\text{F}$ NMR Chemical Shifts Predictions at Different DFT/GIAO Methods and Applying Linear Regression to Improve the Prediction Accuracy

Peng Gao<sup>2†</sup> | Jie Zhang<sup>1\*</sup> | Hongming Chen<sup>1\*</sup>

<sup>1</sup>Centre of Chemistry and Chemical Biology, Guangzhou Regenerative Medicine and Health-Guangdong Laboratory, Guangzhou 53000, China

<sup>2</sup>School of Chemistry and Molecular Bioscience, University of Wollongong, NSW 2500, Australia

## Correspondence

Jie Zhang, Centre of Chemistry and Chemical Biology, Guangzhou Regenerative Medicine and Health-Guangdong Laboratory, Guangzhou 53000, China  
Email: j.chang@mail.ecust.edu.cn

## Funding information

A systematic benchmark of phosphorus and fluorine NMR chemical shifts predictions at six different density functional theory (DFT) / the gauge-including atomic orbital (GIAO) methods was conducted. Two databases were compiled: one consists of 35 phosphorus-containing molecules, which cover the most common intra-molecular bonding environments of trivalent and pentavalent phosphorus atoms; the other is composed of 46 fluorine-containing molecules. The characteristics of each DFT/GIAO method with different solvent models were demonstrated in details. The application of linear regression between the calculated isotropic shielding constants and experimental chemical shifts was applicable to improve the prediction accuracy. And, the best methods with the SMD and CPCM implicit solvent models for  $^{31}\text{P}$  chemical shifts predictions, are able to yield a root-mean-square deviation (RMSDs) of 5.58 ppm and 5.42 ppm, respectively; for  $^{19}\text{F}$ , the corresponding lowest prediction errors with these two applied solvent models are 4.43 ppm and 4.12 ppm. The developed scaling factors fitted from linear regression are applicable to enhance the

chance of successful structural elucidations of phosphorus or **fluorine-containing** compounds, as an efficient complement to  $^{13}\text{C}$ ,  $^1\text{H}$ ,  $^{11}\text{B}$  and  $^{15}\text{N}$  chemical shifts predictions.

#### KEYWORDS

Nuclear Magnetic Resonance Spectroscopy, Density Functional Theory, Gauge-Including Atomic Orbital, Chemical Shift, Linear Regression

## 1 | INTRODUCTION

Accurate yet efficient predictions of nuclear magnetic resonance (NMR) chemical shifts have become more and more important for structural elucidations in modern chemistry research.[1] However, for synthesis or testing work involving phosphorus or **fluorine-containing** species, effective identifications of some intermediate products during fast chemical evolution remains to be challenging merely with  $^{13}\text{C}$  and  $^1\text{H}$  NMR spectroscopy analysis, as the bonding environment of phosphorus atom is usually complicate. The development of an accurate yet affordable computational protocol for  $^{31}\text{P}$  and  $^{19}\text{F}$  NMR chemical shifts predictions can help narrow the structural possibilities for challenging synthesis work, which involves phosphorus or fluorine chemistry.[2, 3, 4, 5, 6, 7, 8, 9, 10, 11, 12]

Quantum calculations of NMR chemical shifts were contributed by Ramsey in 1950s,[13] and due to the development of high-performance computing and the progress in methodology, calculations of isotropic shielding constants have become available with introduction of gauge-including atomic orbital (GIAO) approach.[14] In the recent years, to improve the accuracy and reliability of NMR chemical shifts calculation, various methodological improvements have been conducted. However, the chemical shift of a target atom largely depends on its intra-molecular environment, especially the bonding environment; therefore, many factors may impact the calculation accuracy of such a quantity. The detailed sources of error mainly include electron correlations,[15] solvation effects,[16] vibrational averaging,[17] conformational variations,[18] and heavy atom effects.[19] Different DFT/GIAO methods may display specific advantages to reduce corresponding errors for this kind of calculation, however, for accurate  $^{31}\text{P}$  and  $^{19}\text{F}$  NMR calculations, a systematic benchmark at different methods is necessary.

And beyond a systematic comparison of different computational methods, numerical tools are also helpful to correct the calculated results with respect to experimental values. The application of the empirical scaling factors fitted from the linear regression between the calculated isotropic constants and experimental chemical shifts is a straightforward approach to reduce prediction errors. And in our previous studies, we found that the prediction accuracy for  $^{15}\text{N}$  and  $^{11}\text{B}$  NMR chemical shifts can be largely improved via applying such a correction with merely a modest increase of computational cost. The inclusion of such a numerical correction can overcome errors from an overall perspective, and make complementary to methodological limitations. The fitted slope can scale the calculated isotropic shielding constants, and efficiently reduce systematic errors; while the intercept corresponds to the choice of a reference compound, via which the real values of chemical shifts are defined.

In this study, we first compiled two databases of phosphorous and **fluorine-containing** molecules; and run NMR GIAO calculations with six widely used DFT/GIAO methods. Second, we benchmarked the prediction accuracies of  $^{31}\text{P}$  and  $^{19}\text{F}$  NMR chemical shifts at these applied methods, without and with linear regression corrections, respectively. Through a systematic comparison, the performance of each method was demonstrated. The encouraging consistency with respect to experimental values via linear regression implies a broader application of these two protocols in struc-

tural elucidations. Moreover, the raise of these two protocols are also consistent with previous studies on  $^{13}\text{C}$ ,  $^1\text{H}$ ,  $^{15}\text{N}$  and  $^{11}\text{B}$  NMR chemical shifts; and therefore, for future users, all the predictions can be realized in one set of calculation.

## 2 | METHODOLOGY

### 2.1 | Computational procedure and details

In this study, we first conducted a systematic accuracy benchmarking at six different DFT/GIAO methods with two implicit solvent models for  $^{31}\text{P}$  and  $^{19}\text{F}$  NMR chemical shifts predictions; and then we developed the linear regression scaling factors for more accurate predictions. There are two steps for NMR calculations: first, we conducted geometry optimisations of the collected molecules to locate the minima on their potential energy surfaces in the gas phase. The inclusion of solvent model in this step will be computationally expensive, and the accuracy may not be largely improved.[20] And moreover, these optimised conformations need to be confirmed via vibrational frequency calculations. Second, the NMR calculations in chloroform with both the SMD[21] and CPCM[22] implicit solvent models were conducted to obtain the calculated isotropic shielding constants. It was found that the addition of an implicit solvent model in the second step can largely improve the calculation accuracy of  $^1\text{H}$  and  $^{13}\text{C}$  chemical shifts with merely a small increase of computational cost.[23, 1, 24] However, it was also reported that the inclusion of an explicit solvent model may further improve the calculation accuracy to a higher level,[25, 26] while the required computational cost will be correspondingly larger.

All the calculations were conducted within Gaussian 09.[27] The applications of the first four DFT/GIAO methods (Table 3 and 4, Method 1-4) are to follow the methods proposed by Tantillo and co-workers on  $^1\text{H}$  and  $^{13}\text{C}$  NMR chemical shifts predictions,[23, 1] as well as our previous study focusing on  $^{15}\text{N}$  and  $^{11}\text{B}$  cases.[28, 20] In addition, two additional methods (Table 3 and 4, Method 5 and 6), the performance of which have also been tested for NMR chemical shifts predictions,[28, 20, 29, 30, 31] were also included in this study for a systematic comparison.

### 2.2 | Database of phosphorus and fluorine containing molecules

The database of phosphorus-containing molecules contains 36 molecules with experimental chemical shifts in total; and for fluorine, the database consists of 46 molecules. (see Support Information for more details).[32] The range of  $^{31}\text{P}$  NMR chemical shifts is from -163.5 to 186 ppm; and for  $^{19}\text{F}$ , from -195.1 to 42 ppm. In this study, we focused on trivalent and pentavalent (with similar structures to phosphoric acid) phosphorus atoms, which can form symmetric bonding environment. And considering the linear regression of the calculated isotropic shielding constants with respect to experimental values, we also prefer to small molecules with relatively rigid skeletons to avoid conformational effects. However, the fitted scaling factors are still applicable for the conformers of flexible molecules, provided that the geometry optimisations of these conformers were conducted accurately.[1]

### 2.3 | Linear regression

The linear regressions of the calculated isotropic shielding constants ( $\sigma$ ) at the eight different DFT/GIAO methods can be fitted with the experimental chemical shifts ( $\delta$ ) via the following equation:

$$\delta = \frac{\text{intercept} - \sigma}{-\text{slope}}. \quad (1)$$

Once these scaling factors are obtained, they can be applied to predict the  $^{31}\text{P}$  and  $^{19}\text{F}$  chemical shifts of new molecules.

## 3 | RESULTS AND DISCUSSION

### 3.1 | Benchmark of the predictions accuracy at the adopted methods

Based on the results listed in Table 1 and 2, we can see that among the six methods, Method 6 with geometry optimisation at B3LYP/cc-pVDZ in the gas phase and NMR GIAO calculations at B3LYP/cc-pVDZ with the implicit solvent model, was proved to be most accurate, with a RMSD of 10.90 and 7.98 ppm, for  $^{31}\text{P}$  and  $^{19}\text{F}$ , respectively. And the other 5 methods display comparable performances, with RMSDs ranging from 15.09 to 24.22 and from 14.32 to 20.59 ppm, for  $^{31}\text{P}$  and  $^{19}\text{F}$ , respectively. Moreover, the two methods for NMR GIAO calculations, PBE0 and mPW1PW91, also display similar accuracy for  $^{31}\text{P}$  NMR chemical shift predictions; and PBE0 performs slightly better than mPW1PW91 in  $^{31}\text{F}$  NMR chemical shift predictions (see Method 1 vs 3, and 2 vs 4).

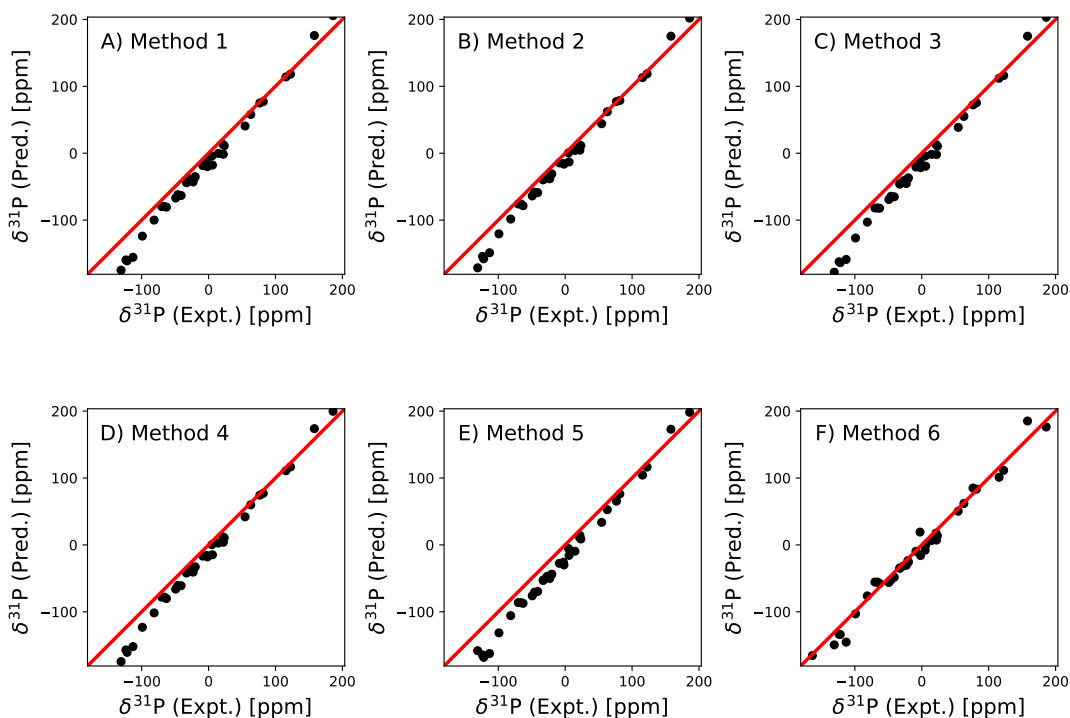


**FIGURE 1** The comparison between the predicted and experimental  $^{31}\text{P}$  NMR chemical shifts. Method 1 to 6 are listed in Table 3, the SMD solvent model was applied.

For the two adopted implicit solvent models, SMD and CPCM, we found that for both  $^{31}\text{P}$  and  $^{19}\text{F}$  NMR chemical

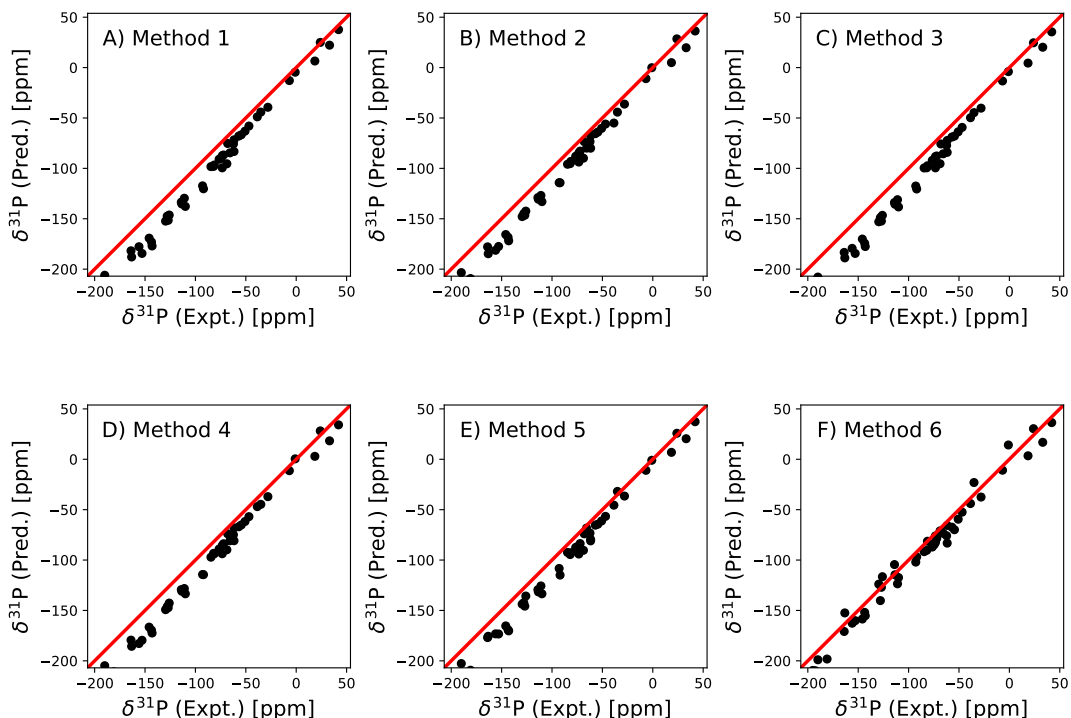


**FIGURE 2** The comparison between the predicted and experimental  $^{31}\text{P}$  NMR chemical shifts. Method 1 to 6 are listed in Table 4, the SMD solvent model was applied.

shifts calculations, the performance of the CPCM model is better than the SMD model. We believe that the addition of implicit solvent model in the optimisation step may further improve the prediction accuracy. However, considering the increased computational costs and corresponding improvement in accuracy, we still recommend to conduct geometry optimisation in the gas phase, and only include the implicit solvent model in the NMR single point calculation step. For the addition of explicit solvent molecules, the computational cost will be extremely large for hundreds of sets of calculations, therefore, the effects of explicit solvent are not investigated in this study.

From Figure 1 and 2, it can be seen that for all the first five methods, their predicted  $^{31}\text{P}$  and  $^{19}\text{F}$  NMR chemical shifts are largely deviated from experimental values. However, the predicted values are linearly distributed, therefore, the application of a linear regression model can be expected to reduce the prediction errors.

**TABLE 1** The performance of the the six DFT/GIAO methods for  $^{31}\text{P}$  NMR chemical shifts predictions.

Method	SMD			CPCM		
	RMSD <sup>a)</sup>	R <sup>2b)</sup>	RMSD <sup>c)</sup>	RMSD <sup>a)</sup>	R <sup>2b)</sup>	RMSD <sup>c)</sup>
1	20.09	0.9946	5.92	17.93	0.9950	5.72
2	17.10	0.9951	5.61	15.09	0.9955	5.42
3	21.86	0.9946	5.89	19.61	0.9950	5.70
4	18.80	0.9951	5.64	16.74	0.9954	5.68
5	24.22	0.9952	5.58	21.86	0.9952	5.56
6	11.56	0.9835	10.41	10.90	0.9838	10.29

<sup>a)</sup> RMSD for the calculated chemical shifts of **phosphorus-containing** molecules included in the database with respect to their experimental values (in ppm) (see Table. S.4 in Support Information) without corrections by linear regression. <sup>b)</sup> The value of R<sup>2</sup> represents the coefficient of determination for the linear regression. <sup>c)</sup> RMSD for the calculated chemical shifts of **phosphorus-containing** molecules included in the database with respect to their experimental values (in ppm) (see Table. S.4 in Support Information) with corrections by linear regression.

**TABLE 2** The performance of the the six DFT/GIAO methods for  $^{19}\text{F}$  NMR chemical shifts predictions.

Method	SMD			CPCM		
	RMSD <sup>a)</sup>	R <sup>2b)</sup>	RMSD <sup>c)</sup>	RMSD <sup>a)</sup>	R <sup>2b)</sup>	RMSD <sup>c)</sup>
1	19.77	0.9940	4.59	18.19	0.9950	4.21
2	16.77	0.9942	4.51	15.08	0.9955	4.18
3	20.59	0.9942	4.51	19.00	0.9952	4.12
4	17.47	0.9942	4.43	16.24	0.9943	4.49
5	15.61	0.9927	5.08	14.32	0.9938	4.67
6	10.15	0.9824	7.92	9.38	0.9821	7.98

<sup>a)</sup> RMSD for the calculated chemical shifts of **fluorine-containing** molecules included in the database with respect to their experimental values (in ppm) (see Table S.1 in Support Information) without corrections by linear regression. <sup>b)</sup> The value of R<sup>2</sup> represents the coefficient of determination for the linear regression. <sup>c)</sup> RMSD for the calculated chemical shifts of **fluorine-containing** molecules included in the database with respect to their experimental values (in ppm) (see Table S.1 in Support Information) with corrections by linear regression.

**TABLE 3** The six methods adopted for calculating  $^{31}\text{P}$  isotropic shielding constants and the fitted empirical scaling parameters (slope and intercept) in Chloroform.

Method	Geometry <sup>a)</sup> (opt & freq)	NMR <sup>b)</sup> (GIAO)	SMD <sup>c)</sup>		CPCM <sup>d)</sup>	
			slope	intercept	slope	intercept
1	B3LYP/6-31+G(d,p)	mPW1PW91/6-311+G(2d,p)	-1.1446	303.83	-1.1364	303.66
2	B3LYP/6-311+G(2d,p)	mPW1PW91/6-311+G(2d,p)	-1.2777	307.74	-1.1199	307.57
3	B3LYP/6-31+G(d,p)	PBE0/6-311+G(2d,p)	-1.1488	307.43	-1.1404	307.25
4	B3LYP/6-311+G(2d,p)	PBE0/6-311+G(2d,p)	-1.1322	311.16	-1.1244	311.02
5	B3LYP/cc-pVDZ	mPW1PW91/6-311+G(2d,p)	-1.1431	297.77	-1.1336	297.48
6	B3LYP/cc-pVDZ	B3LYP/cc-pVDZ	-1.0265	373.81	-1.0199	373.60

<sup>a)</sup> Both the geometry optimisation and vibrational frequency calculation were conducted using this method. <sup>b)</sup> The NMR GIAO calculation [14] was conducted using this method with inclusion of the implicit solvent model. <sup>c)</sup> The developed scaling factors from linear regression (slope and intercept in Eq. 1) for  $^{31}\text{P}$  NMR chemical shifts predictions with the SMD model.[21] The scaled  $^{31}\text{P}$  NMR chemical shifts were present in Figure 3. <sup>d)</sup> The developed scaling factors from linear regression (slope and intercept in Eq. 1) for  $^{31}\text{P}$  NMR chemical shifts predictions with the CPCM model.[22] The scaled  $^{31}\text{P}$  NMR chemical shifts were present in Support Information.

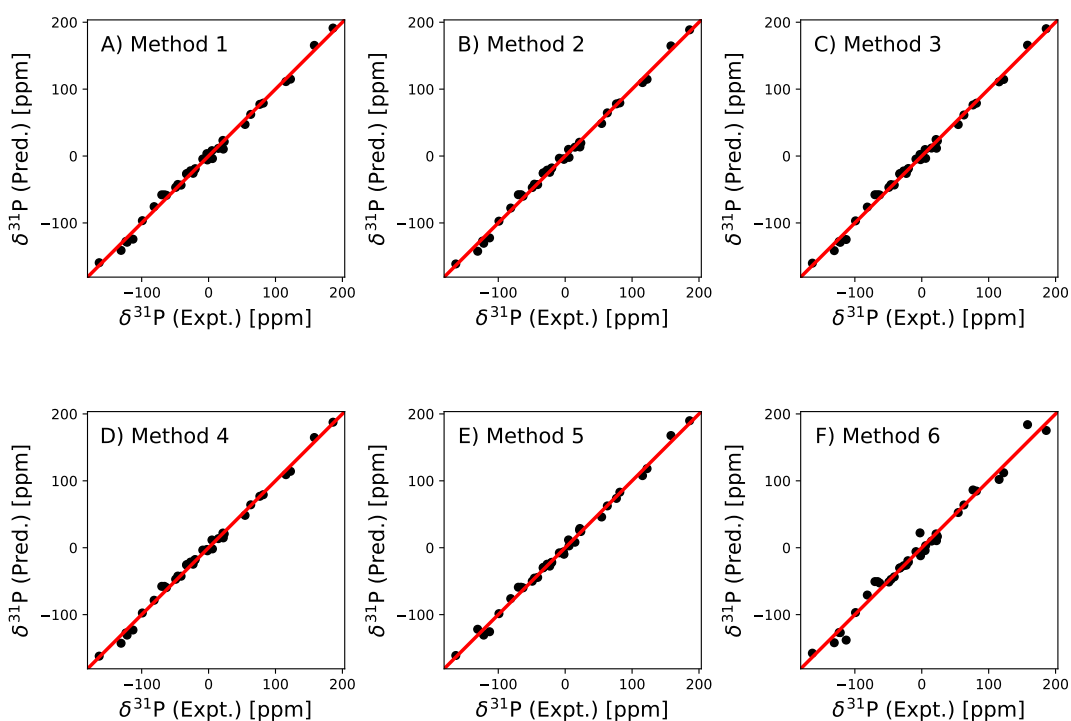
**TABLE 4** The six methods adopted for calculating  $^{19}\text{F}$  isotropic shielding constants and the fitted empirical scaling parameters (slope and intercept) in Chloroform.

Method	Geometry <sup>a)</sup> (opt & freq)	NMR <sup>b)</sup> (GIAO)	SMD <sup>c)</sup>		CPCM <sup>d)</sup>	
			slope	intercept	slope	intercept
1	B3LYP/6-31+G(d,p)	mPW1PW91/6-311+G(2d,p)	-1.1109	167.47	-1.1079	167.00
2	B3LYP/6-311+G(2d,p)	mPW1PW91/6-311+G(2d,p)	-1.0940	173.02	-1.0949	171.96
3	B3LYP/6-31+G(d,p)	PBE0/6-311+G(2d,p)	-1.1111	166.94	-1.1092	166.37
4	B3LYP/6-311+G(2d,p)	PBE0/6-311+G(2d,p)	-1.0979	171.97	-1.0936	171.86
5	B3LYP/cc-pVDZ	mPW1PW91/6-311+G(2d,p)	-1.0852	170.90	-1.0842	170.55
6	B3LYP/cc-pVDZ	B3LYP/cc-pVDZ	-1.0165	189.42	-1.0134	188.85

<sup>a)</sup> Both the geometry optimisation and vibrational frequency calculation were conducted using this method. <sup>b)</sup> The NMR GIAO calculation [14] was conducted using this method with inclusion of the implicit solvent model. <sup>c)</sup> The developed scaling factors from linear regression (slope and intercept in Eq. 1) for  $^{19}\text{F}$  NMR chemical shifts predictions with the SMD model.[21] The scaled  $^{19}\text{F}$  NMR chemical shifts were present in Figure 4. <sup>d)</sup> The developed scaling factors from linear regression (slope and intercept in Eq. 1) for  $^{19}\text{F}$  NMR chemical shifts predictions with the CPCM model.[22] The scaled  $^{19}\text{F}$  NMR chemical shifts were present in Support Information.

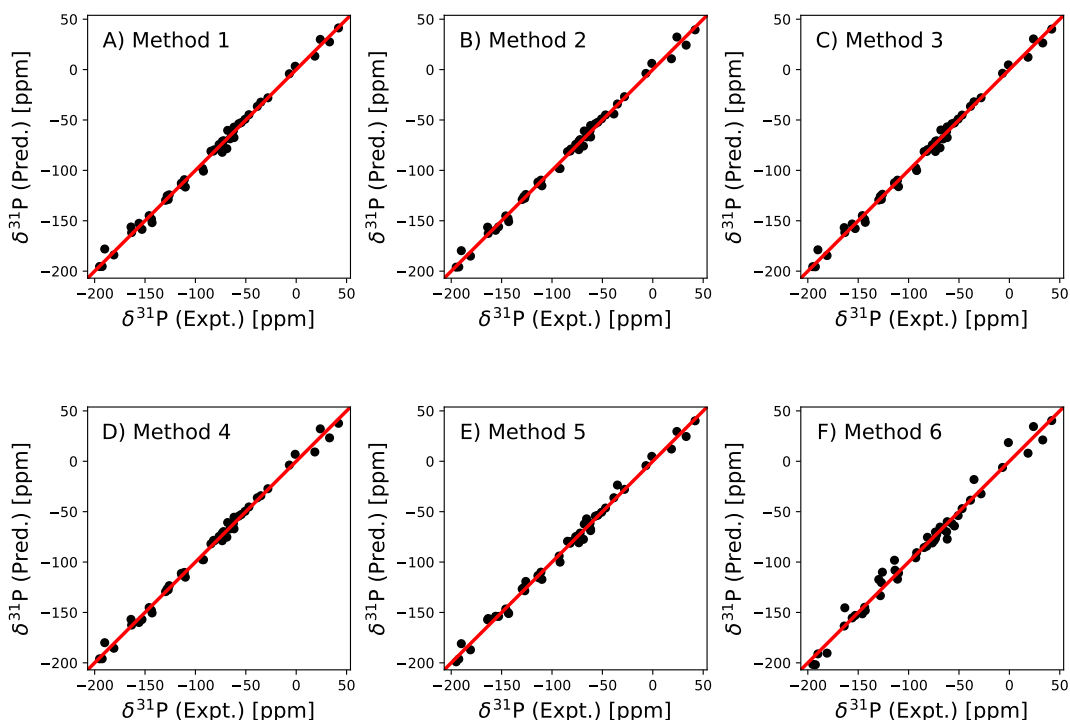
## 3.2 | The accuracy improvement with linear regression model

Figure 3 and 4 present the linear scaled calculated  $^{31}\text{P}$  isotropic shielding constants with respect to experimental values for all the six DFT/GIAO methods with the SMD implicit model, we can see that the overall accuracy is largely improved for the first five methods, compared to pure DFT/GIAO calculations. The RMSDs were reduced to less than 6 and 5 ppm for  $^{31}\text{P}$  and  $^{19}\text{F}$ , respectively (more details will be discussed below). The scaled results with the CPCM model can be found in Support Information. It indicates that the application of scaling factors fitted from linear regression (presented in Table 3 and 4) between the calculated isotropic shielding constants and experimental NMR chemical shifts is a straightforward way to improve the prediction accuracy of  $^{31}\text{P}$  and  $^{19}\text{F}$  NMR chemical shifts with no substantial increase of computational cost. And such a correction has also been successfully applied for  $^{11}\text{B}$ ,  $^1\text{H}$ ,  $^{13}\text{C}$  and  $^{15}\text{N}$  chemical shift predictions in previous studies.[28, 31, 30, 1]



**FIGURE 3** The comparison between the predicted and experimental  $^{31}\text{P}$  NMR chemical shifts. Method 1 to 6 are listed in Table 3, the SMD solvent model was applied, the scaling factors were used for corrections.

For all the six DFT/GIAO methods with inclusion of implicit solvent model, the corresponding values of  $R^2$  were very close to 1.0 (Table 1 and 2) for both  $^{31}\text{P}$  and  $^{19}\text{F}$ , demonstrating that there exists a strong linear regression relationship between the collected experimental data and the DFT calculated isotropic shielding constants. At the same time, the deviation of slope from a value of -1 indicates that linear regression could correct the systematic errors effectively for these adopted DFT/GIAO calculations.[1] From the summarised RMSDs, it can be seen that the per-



**FIGURE 4** The comparison between the predicted and experimental  $^{31}\text{P}$  NMR chemical shifts. Method 1 to 6 are listed in Table 4, the SMD solvent model was applied, the scaling factors were used for corrections.

performances of the first five methods are comparably good. With scaling factors, the errors of their predicted  $^{31}\text{P}$  and  $^{19}\text{F}$  chemical shifts with respect to the experimental data are within the ranges of 5.42–5.92 ppm and 4.12–5.08 ppm, respectively (Table 1 and 2). For  $^{31}\text{P}$ , Method 2 with geometry optimisation at B3LYP/6-311+G(2d,p) and NMR GIAO calculations at mPW1PW91/6-311+G(2d,p) performs best. For  $^{19}\text{F}$ , Method 4 with geometry optimisation at B3LYP/6-311+G(2d,p) and NMR GIAO calculations at PBE0/6-311+G(2d,p) provides the most reliable results. Moreover, one important advantage of these two methods (with the SMD solvent model in NMR GIAO calculation) lies in the fact that it could also predict chemical shifts for  $^1\text{H}$ ,  $^{13}\text{C}$ ,  $^{15}\text{N}$  and  $^{11}\text{B}$  with a consistent accuracy. Therefore, with corresponding scaling factors, all kinds of chemical shifts can be predicted accurately in one set of calculation. We recommend the application of the scaling factors fitted from Method 2 and 4 for potential researchers. For Method 6, the linear regression cannot improve its prediction accuracy to a large degree. However, considering its effectiveness in predicting  $^{31}\text{P}$  and  $^{19}\text{F}$  NMR chemical shifts without linear regression, we still recommend it to be applied for experimental researchers.

For the two applied implicit solvent models, SMD and CPCM, we noticed that with linear regression even their performance for both  $^{31}\text{P}$  and  $^{19}\text{F}$  NMR chemical shifts predictions, are all improved (see details in Table 1 and 2); however, the CPCM model is still better than the SMD model, consistent with our discussion of the pure performance of the six DFT/GIAO methods without linear regression. *It is worth noting that, the SMD model has already been ap-*

plied to fit the scaling factors for  $^1\text{H}$ ,  $^{13}\text{C}$ ,  $^{15}\text{N}$  and  $^{11}\text{B}$  chemical shifts predictions, and the CPCM model has only been applied for  $^{11}\text{B}$  case. Therefore, currently, we recommend to include the SMD model in the NMR GIAO calculation step for  $^{31}\text{P}$  and  $^{19}\text{F}$  NMR chemical shifts predictions. Hopefully, in the near future, another complete set of scaling factors for various NMR chemical shifts predictions can be developed with the CPCM model.

## 4 | CONCLUSION

A systematic benchmarking study of  $^{31}\text{P}$  and  $^{19}\text{F}$  NMR chemical shifts predictions at six DFT/GIAO methods with two implicit solvent models has been conducted. The scaling factors fitted from the linear regression between the calculated isotropic shielding constants and the experimental NMR chemical shifts have also been applied to improve the predictions accuracy of  $^{31}\text{P}$  and  $^{19}\text{F}$  NMR chemical shifts. Such a procedure is first proposed by Tantillo and co-workers[23, 1], and is consistent with our previous studies focusing on  $^{11}\text{B}$  and  $^{15}\text{N}$  chemical shifts predictions.[28, 20] And, we noticed that for both  $^{31}\text{P}$  and  $^{19}\text{F}$  cases, the overall accuracy was largely improved via applying the scaling factors, compared to that of the pure DFT/GIAO methods. And among the six methods, Method 2 with geometry [optimisation](#) at B3LYP/6-311+G(2d,p) and NMR GIAO calculation at mPW1PW91/6-311+G(2d,p) provide the most reliable predictions for  $^{31}\text{P}$  chemical shifts predictions. And for  $^{19}\text{F}$ , Method 4 with geometry [optimisation](#) at B3LYP/6-311+G(2d,p) and NMR GIAO calculation at PBE0/6-311+G(2d,p) performs best. And we hope that these two protocols raised in this study could work together with the ones on  $^1\text{H}$ ,  $^{13}\text{C}$ ,  $^{15}\text{N}$  and  $^{11}\text{B}$  chemical shifts predictions to serve as a complete tool for challenging structural elucidations in chemical research. However, it also needs to be underscored that if the trivalent or pentavalent phosphorous atoms are bonded with heavy atoms (this kind of phosphorous containing molecules were excluded from our current database), the corresponding prediction errors will be much larger, and cannot be reduced effectively via simple linear regression. [Such an error](#) is likely due to the asymmetric distribution of electron density and has also been noted in  $^{15}\text{N}$  and  $^{13}\text{C}$  chemical shift studies. Therefore, the deficiency of the adopted DFT method for this kind of calculations remain to be investigated in future study.[1]

## acknowledgements

We wish to thank the Australian Government for providing an Australian International Postgraduate Award scholarship for P.G to complete his PhD degree. And, we also thank Dr. Jun Zhang for helpful discussions. And the some of the computational work was undertaken at the National Computational Merit Allocation Scheme supported by the Australian Government (Project id: v15).

## conflict of interest

There is no conflict of interest.

## Supporting Information

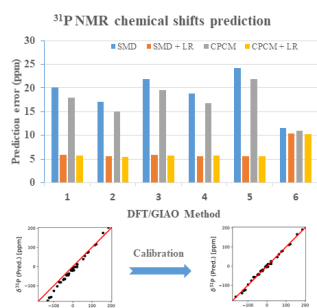
Related experimental and calculated data can be founded in Supporting Information.

## references

- [1] Lodewyk MW, Siebert MR, Tantillo DJ. Computational Prediction of  $^1\text{H}$  and  $^{13}\text{C}$  Chemical Shifts: A Useful Tool for Natural Product, Mechanistic, and Synthetic Organic Chemistry. *Chemical Reviews* 2012 mar;112(3):1839–1862.
- [2] Eichele K, Wasylishen RE, Kessler JM, Solujić L, Nelson JH. Phosphorus Chemical Shift Tensors of Phosphole Derivatives Determined by  $^{31}\text{P}$  NMR Spectroscopy of Powder Samples. *Inorganic Chemistry* 1996;35(13):3904–3912.
- [3] Lin YC, Hatzakis E, McCarthy SM, Reichl KD, Lai TY, Yennawar HP, et al. P–N Cooperative Borane Activation and Catalytic Hydroboration by a Distorted Phosphorous Triamide Platform. *Journal of the American Chemical Society* 2017;139(16):6008–6016.
- [4] Ackermann M, Pascariu A, Höcher T, Siehl HU, Berger S. Electronic Properties of Furyl Substituents at Phosphorus and Their Influence on  $^{31}\text{P}$  NMR Chemical Shifts. *Journal of the American Chemical Society* 2006;128(26):8434–8440.
- [5] Tropp J, Blumenthal NC, Waugh JS. Phosphorus NMR study of solid amorphous calcium phosphate. *Journal of the American Chemical Society* 1983;105(1):22–26.
- [6] Smith ICP, Jarrell HC. Deuterium and phosphorus NMR of microbial membranes. *Accounts of Chemical Research* 1983;16(8):266–272.
- [7] Howe PWA. Recent developments in the use of fluorine NMR in synthesis and characterisation. *Progress in Nuclear Magnetic Resonance Spectroscopy* 2020;118-119:1 – 9. <http://www.sciencedirect.com/science/article/pii/S0079656520300108>.
- [8] Dahanayake JN, Kasireddy C, Ellis JM, Hildebrandt D, Hull OA, Karnes JP, et al. Evaluating electronic structure methods for accurate calculation of  $^{19}\text{F}$  chemical shifts in fluorinated amino acids. *Journal of Computational Chemistry* 2017;38(30):2605–2617.
- [9] Saielli G, Bini R, Bagno A. Computational  $^{19}\text{F}$  NMR. 2. Organic compounds. *RSC Adv* 2014;4:41605–41611.
- [10] Lau EY, Gerig JT. Origins of Fluorine NMR Chemical Shifts in Fluorine-Containing Proteins. *Journal of the American Chemical Society* 2000;122(18):4408–4417.
- [11] Urlick AK, Calle LP, Espinosa JF, Hu H, Pomerantz WCK. Protein-Observed Fluorine NMR Is a Complementary Ligand Discovery Method to  $^1\text{H}$  CPMG Ligand-Observed NMR. *ACS Chemical Biology* 2016;11(11):3154–3164.
- [12] Dalvit C, Vulpetti A. Ligand-Based Fluorine NMR Screening: Principles and Applications in Drug Discovery Projects. *Journal of Medicinal Chemistry* 2019;62(5):2218–2244.
- [13] Pyykkö P. Perspective on Norman Ramseys theories of NMR chemical shifts and nuclear spin-spin coupling. *Theoretical Chemistry Accounts* 2000 feb;103(3-4):214–216.
- [14] Ditchfield R. Self-consistent perturbation theory of diamagnetism. *Molecular Physics* 1974 apr;27(4):789–807.
- [15] Gauss J, Stanton JF. Electron-Correlated Approaches for the Calculation of NMR Chemical Shifts. In: Prigogine I, Rice SA, editors. *Advances in Chemical Physics* John Wiley & Sons, Inc.; 2003.p. 355–422.
- [16] Dracinsky M, Bour P. Computational Analysis of Solvent Effects in NMR Spectroscopy. *Journal of Chemical Theory and Computation* 2010 jan;6(1):288–299.
- [17] Helgaker T, Jaszuriski M, Ruud K. Ab Initio Methods for the Calculation of NMR Shielding and Indirect Spin-Spin Coupling Constants. *Chemical Reviews* 1999 jan;99(1):293–352.
- [18] Barone G, Duca D, Silvestri A, Gomez-Paloma L, Riccio R, Bifulco G. Determination of the Relative Stereochemistry of Flexible Organic Compounds by Ab Initio Methods: Conformational Analysis and Boltzmann-Averaged GIAO  $^{13}\text{C}$  NMR Chemical Shifts GIAO=gauge including atomic orbitals. *Chemistry - A European Journal* 2002 jul;8(14):3240–3245.

- [19] Kaupp M, Malkina OL, Malkin VG, Pyykkö P. How Do Spin-Orbit-Induced Heavy-Atom Effects on NMR Chemical Shifts Function? Validation of a Simple Analogy to Spin-Spin Coupling by Density Functional Theory (DFT) Calculations on Some Iodo Compounds. *Chemistry - A European Journal* 1998 jan;4(1):118–126.
- [20] Gao P, Wang X, Huang Z, Yu H.  $^{11}\text{B}$  NMR Chemical Shift Predictions via Density Functional Theory and Gauge-Including Atomic Orbital Approach: Applications to Structural Elucidations of Boron-Containing Molecules. *ACS Omega* 2019;4(7):12385–12392.
- [21] Marenich AV, Cramer CJ, Truhlar DG. Universal Solvation Model Based on Solute Electron Density and on a Continuum Model of the Solvent Defined by the Bulk Dielectric Constant and Atomic Surface Tensions. *The Journal of Physical Chemistry B* 2009 may;113(18):6378–6396.
- [22] Barone V, Cossi M. Quantum Calculation of Molecular Energies and Energy Gradients in Solution by a Conductor Solvent Model. *The Journal of Physical Chemistry A* 1998;102(11):1995–2001.
- [23] CHESHIRE CCAT, the Chemical Shift Repository for computed NMR scaling factors, with Coupling Constants Added Too.; 2017. <http://cheshirenmr.info/index.htm>.
- [24] Jain R, Bally T, Rablen PR. Calculating Accurate Proton Chemical Shifts of Organic Molecules with Density Functional Methods and Modest Basis Sets. *The Journal of Organic Chemistry* 2009 jun;74(11):4017–4023.
- [25] Zhu T, Zhang JZH, He X. Automated Fragmentation QM/MM Calculation of Amide Proton Chemical Shifts in Proteins with Explicit Solvent Model. *Journal of Chemical Theory and Computation* 2013 mar;9(4):2104–2114.
- [26] Exner TE, Frank A, Onila I, Möller HM. Toward the Quantum Chemical Calculation of NMR Chemical Shifts of Proteins. 3. Conformational Sampling and Explicit Solvents Model. *Journal of Chemical Theory and Computation* 2012;8(11):4818–4827.
- [27] Frisch MJ, Trucks GW, Schlegel HB, Scuseria GE, Robb MA, Cheeseman JR, et al., Gaussian 09 Revision E.01.; Gaussian Inc. Wallingford CT 2009.
- [28] Gao P, Wang X, Yu H. Towards an Accurate Prediction of Nitrogen Chemical Shifts by Density Functional Theory and Gauge-Including Atomic Orbital. *Advanced Theory and Simulations* 2019;2:1800148.
- [29] Gao P, Zhang J, Peng Q, Zhang J, Glezakou VA. General Protocol for the Accurate Prediction of Molecular  $^{13}\text{C}/^{1}\text{H}$  NMR Chemical Shifts via Machine Learning Augmented DFT. *Journal of Chemical Information and Modeling* 2020;xxx(xxx):xxx.
- [30] Xin D, Sader CA, Fischer U, Wagner K, Jones PJ, Xing M, et al. Systematic investigation of DFT-GIAO  $^{15}\text{N}$  NMR chemical shift prediction using B3LYP/cc-pVDZ: application to studies of regioisomers, tautomers, protonation states and N-oxides. *Organic Biomolecular Chemistry* 2017;15(4):928–936.
- [31] Xin D, Sader CA, Chaudhary O, Jones PJ, Wagner K, Tautermann CS, et al. Development of a  $^{13}\text{C}$  NMR Chemical Shift Prediction Procedure Using B3LYP/cc-pVDZ and Empirically Derived Systematic Error Correction Terms: A Computational Small Molecule Structure Elucidation Method. *The Journal of Organic Chemistry* 2017;82(10):5135–5145.
- [32] Structure Determination Using Spectroscopic Methods.; 2017. <https://www.chem.wisc.edu/areas/reich/nmr/>.

## GRAPHICAL ABSTRACT



The prediction errors of  $^{31}\text{P}$  and  $^{19}\text{F}$  NMR chemical shifts have been largely reduced via the application of empirical scaling factors.